Design and Optimization of Copper Zinc Tin Sulfide (CZTS) Thin Film Solar Cell

Hafizur Rahman Alve[1‡], Md Hasibur Rahman[2], Md Emdadul Ahsan[3], Mrinmoy Dey[1]

[1]Department of Electrical and Electronic Engineering, Chittagong University of Engineering and Technology, Chattogram-4349, Bangladesh

[2]Department of Materials Science and Engineering, Rajshahi University of Engineering and Technology, Rajshahi- 6204, Bangladesh

[3]Department of Microelectronic Science and Engineering, Yangzhou University, Yangzhou-225000, China

(alve8969@gmail.com, hasibemon82@gmail.com, ahsan.shaheb1@outlook.com, mrinmoy@cuet.ac.bd)

[‡]Corresponding Author; Hafizur Rahman Alve, Department of Electrical and Electronic Engineering, Chittagong University of Engineering and Technology, Chattogram- 4349, Bangladesh, Tel: +8801645084581, alve8969@gmail.com

Received: 11.07.2024 Accepted: 26.08.2024

Abstract- In this research work, we show how to develop and simulate highly efficient Copper Zinc Tin Sulfide (CZTS) based thin film solar cell with dual-heterojunction. A dual-heterojunction is created when Copper Zinc Tin Sulfide (CZTS) forms a p-n junction with a window layer and another p-p$^+$ connection with a highly doped back surface Field (BSF) layer. The simulation was performed with SCAPS-1D software, which uses known experimental physical parameters. The results exhibit the best PCE as high as 45.08 % with V_{oc}=1.346 V, J_{sc}=41.59 mA/cm^2, FF=80.49 % for dual heterojunction structure of n-ZnSe/p-CZTS/p$^+$-CGS/Ni with a good level of temperature coefficient (TC) is found to be (-0.069 %/◦C). The simulation results show that the PCE of the single heterojunction n-ZnSe/p-CZTS/Ni solar cell may reach 19.62%, while the Power Conversion Efficiency (PCE) of the dual heterojunction solar cell can reach 45.08 %.

Keywords: Dual-heterojunction; CZTS; BSF; CGS; SCAPS-1D.

Nomenclature

Symbol

W (µm)	Thickness	N_t (eV^{-1}cm^{-3})	Peak defect density
ϵ_r	Dielectric Relative Permittivity	N_V (cm^{-3})	Valance Band Effective Density
χ	Electron Affinity	N_C (cm^{-3})	Conduction Band Effective Density
E_g (eV)	Band Gap	N_d (cm^{-3})	Donor Density
V_{oc} (V)	Open Circuit Voltage	N_a (cm^{-3})	Acceptor Density

Acronyms and Abbreviations

PCE	Power Conversion Efficiency
BSF	Back Surface Field
ZnSe	Zinc Selenide
CZTS	Copper Zinc Tin Sulfide
CGS	Copper Gallium Selenide

J_{sc} (mA/cm^2)	Short Circuit Current	μ_e (cm^{-2}/Vs)	Electron Mobility	Ti	Titanium
FF (%)	Fill Factor	μ_h (cm^{-2}/Vs)	Hole Mobility	Ni	Nickel
η (%)	Efficiency	T (K)	Temperature		

1. Introduction

The basis for solar energy and photovoltaic (PV) technology is the notion that sunlight is tapped into to create useful energy types. This procedure furthermore calls for solar radiation collection to transform how much sun oriented radiation into helpful types of energy like heat and electricity. Solar energy has no fossil fuel by products and is really great for the climate. For solar photovoltaic, crystalline silicon (c-Si) technology currently has the bulk of market share (PV). Monocrystalline crystals are the first category. To create the polycrystalline form of silicon, a block of cast silicon must first be divided into bars. In addition to the crystalline silicon-based technology.PV tools and supplies can be used to convert solar energy into electrical power. A solar gadget is made up of one single cell. Photovoltaic (PV) cells have a restricted power output and are usually relatively tiny. These phones, which are typically constructed from a range of semiconductor materials, are thinner than four human hairs. Cells are encased in a mix of polymers and/or glass and positioned between two layers of protection to guarantee that they can withstand the environment for an extended period of time. PV cells are frequently connected to bigger units known as modules or boards in order to improve the amount of power they can generate. To generate arrays, modules can be utilized alone or in combination with other modules. Due to its notable power conversion efficiency (PCE), a range of solar cells made of various materials and manufacturing techniques have become more and more popular recently. These include solar cells made of zinc telluride (Zn_3P_2), copper indium gallium selenide (CIGS), and cadmium telluride (CdTe) [1]. Distinguished by its unique hue, monocrystalline solar cells are the purest form of silicon cells, with confirmed efficiency over 20 % [2]. However, due of their four-sided cutting method, they are quite costly. Polycrystalline solar cells, which are produced by the plasma-enhanced chemical vapor deposition (PECVD) method, have been offered as a more affordable option [3]. They record an efficiency of around 15.5 %, which is lower than their efficiency, and they are also less resilient to temperature variations [4].

Thin-film solar cells, which are distinguished by their layered construction, have been available for purchase since about 2002 [5]. But they are still quite expensive and have poor efficiency. CdTe solar cells, which have an efficiency of 11% on record, were created in an attempt to lower the cost of solar cells, despite their toxicity [6]. The structural and optical features indicate that the produced CdTe films can serve as an appropriate absorber layer for thin film-based solar cells [7, 8, 9]. Researchers conducted research on absorber materials, as well as window layer and buffer layer materials, for the appropriate solar cell structure [10, 11, 12, 13]. As a result, attention has been drawn to Copper Zinc Tin Sulfide (CZTS) solar cells, which are inexpensive, extremely effective, and safe for the environment. Researchers performed research on best hetero-junction partner of CZTS to boost up PCE, better thermal stability as well as preserve the potential photovoltaic materials in earth crust [14, 15, 16]. CZTS quaternary semiconductors have garnered particular attention as thin-film solar cells since the late 2000s. The naturally occurring, non-toxic CZTS has been shown to have an efficiency of 9.2 % when paired with a $Zn_{1-x}Cd_xS$ window layer [17]. The goal of current research is to lower the cost and increase the efficiency of CZTS solar cells. The chemical formula of CZTS is Cu_2ZnSnS_4, and it has the appearance of greenish-black crystals with a density of 4.59 g/cm³ and a molar mass of 439.471 g/mol [18]. Its tetragonal crystal structure, 1.4–1.5 eV band gap, and melting point of 990°C all point to its feasible fabrication and long-term durability [19]. With an absorption value of 10^4 cm^{-1}, CZTS offers various benefits as an absorber layer that enable it to absorb more photons and convert them into electrical energy [20]. Furthermore, CZTS has a dielectric constant of 13.65 and a high relative permittivity of around 10, indicating that it polarizes more readily and converts light into electrical energy more efficiently [21, 22]. The disorder of Cu–Zn cations, a typical defect shown by neutron scattering, is one of CZTS's main disadvantages. This problem affects the PCE of CZTS solar cells by causing a significant open-circuit voltage deficit [23]. Because of the electron trapping states these flaws produce, recombination is facilitated, lowering the open-circuit voltage and the solar cell's efficiency [24]. But, temperature therapy can lessen this issue [25]. Other ways to get over CZTS absorber layer flaws include choosing the right back contact to increase electrical conductivity, annealing in a vacuum to improve crystal quality, and keeping the thickness of the layer less than 2500 nm to minimize ohmic contact [26].

Based on the Shockley–Queisser detailed-balance theory, a dual-heterojunction solar cell can have a maximum efficiency of between 42% and 46% [27, 28]. A three-terminal dual-heterojunction bipolar transistor solar cell with a theoretical efficiency potential of around 54.7% has been claimed by Marti et al. [29]. This activity involves designing and simulating a highly efficient Cu_2ZnSnS_4 (CZTS)-based solar cell. Cu_2ZnSnS_4 (CZTS)-based solar cells have previously been the subject of extensive study; the cell structure of n-ZnS/p-CZTS/p^+-WSe_2 with V_{oc}=0.96V, J_{sc}=33.72 mA/cm², FF=83.75 %, and a PCE of 27.31 was determined to have the latest best performance [30].

The main objective and aim of this work is to modeling Copper Zinc Tin Sulfide (CZTS) based thin film solar cell with best performance and more stable cell structure. For this, dual heterojunction cell structure is introduced which is the novelty of this research work. The methodology of dual-heterojunction is that the absorber layer forms a p-n junction with a window layer and another p-p^+ connection with a highly doped back surface Field (BSF) layer. As a result, dual-heterojunction is created. Firstly, in order to determine the ideal window layer structure, we examine the performance of ZnSe window layer with the change in value of thicknesses and doping concentration. Secondly, as a back surface field (BSF) layer, we used copper gallium selenide (CGS) and we assessed the performance according to thickness and doping concentration. Finally, we built dual-heterojunction solar cell with the cell structure of n-ZnSe/p-CZTS/p^+-CGS/Ni and the power conversion efficiency (PCE) is 45.08 %. So, the optimization of the power conversion efficiency (PCE) was made by this dual heterojunction cell structure. To ensure the stability of this model we analysed temperature effect on the cell structure and find temperature coefficient (TC) is (-0.069 %/◦C) which proves this cell structure is stable.

2. Modeling and Simulation

The simulation was conducted with experimental physical parameters using SCAPS-1D software. SCAPS-1D solves the drift-diffusion equations, Poisson's equation, and continuity equations for electrons and holes in one dimension and uses numerical algorithms like the Finite Difference Method (FDM), Newton-Raphson Method, and Gummel's Method to solve complex equations that describe the behavior of solar cells. Numerical simulations were powered by a single sun with 100 mW/cm^2 of light along with a 1.5G spectrum global air mass (AM). 100 mW/cm^2 means that each square centimeter of the area is receiving 100 milliwatts of power and AM1.5G spectrum is used as a standard for testing solar cells, as it approximates the sunlight conditions in mid-latitude regions. At 300 K, the operational temperature was being measured. There was no consideration of the radiative recombination coefficient, and the optimal values of shunt and series resistance were employed. Bulk layers were assumed to have Gaussian acceptor and donor doping patterns, and interface defects were also investigated.

The simulated schematic design of the dual-heterojunction n-ZnSe/p-CZTS/p^+-CGS/Ni cell is shown in "Figure 1". Nickel (Ni) acts as the back contact in this structure. Incoming sunlight is absorbed by the CGS and CZTS layers, after it has passed through the ZnSe layer. CZTS has an ionization potential of 7.5 eV and an electron affinity of 4.5 eV, whereas ZnSe has an ionization potential of 6.79 eV [31, 32]. Because of this, ZnSe is a good material to use with CZTS to generate a p-n heterojunction. Furthermore, owing to its 1.66 eV band gap and 3.67 eV electron affinity [33], CGS may create a suitable p-p+ heterojunction with CZTS. In the presence of the appropriate energy barriers, the holes created by the CZTS and CGS layers can migrate toward the anode, making it easier for them to reach the cathode.

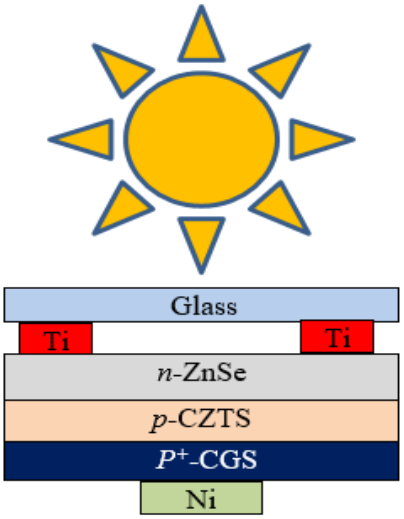

Fig. 1. Proposed structure of CZTS solar cell

Table 1. Electrical parameter of different layers for simulation in SCAPS

Material Properties	ZnSe [31]	CZTS [32]	CGS [33, 34, 35]
W (µm)	0.05	0.8	0.2
E_g (eV)	2.7	1.5	1.66
χ (eV)	4.09	4.5	3.67
ϵ_r	9.2	10	8.5
N_c (cm^3)	1.5×10^{18}	2.2×10^{18}	2.2×10^{17}
N_v (cm^3)	1.8×10^{19}	1.8×10^{19}	1.8×10^{18}
μ_h (cm^2/Vs)	20	25	25
μ_e (cm^2/Vs)	50	100	100
N_a (cm^{-3})	0	1×10^{16}	1.0×10^{19}
N_d (cm^{-3})	1×10^{18}	0	0
Distribution	Gaussian	Gaussian	single
Type of defect	Acceptor	Donor	Donor
N_t (eV^{-1}cm^{-3})	5.642×10^{14}	5.642×10^{14}	1×10^{14}
Reference Energy [eV]	1.350	0.650	0.6

3. Results and Discussion

3.1. ZnSe Window Layer effect on Cell Performance

ZnSe window layer generally has a range of ideal thicknesses that maximize solar cell conversion efficiency. A compromise between carrier collection and light transmission determines the ideal thickness. To successfully capture photon generated carriers and ensure low carrier recombination as well as maximal current extraction, it should be thick enough. It should not, however, be very thick since this may prevent light from reaching the absorber layer, lowering the quantity of incoming light that can be absorbed and resulting in less photo-current production [36]. The conversion ability of a thin film solar cell may be altered by changing thickness of ZnSe window layer. This is essential for aiding effective carrier

collection, lowering recombination losses, and improving the solar cell's overall efficiency [37].

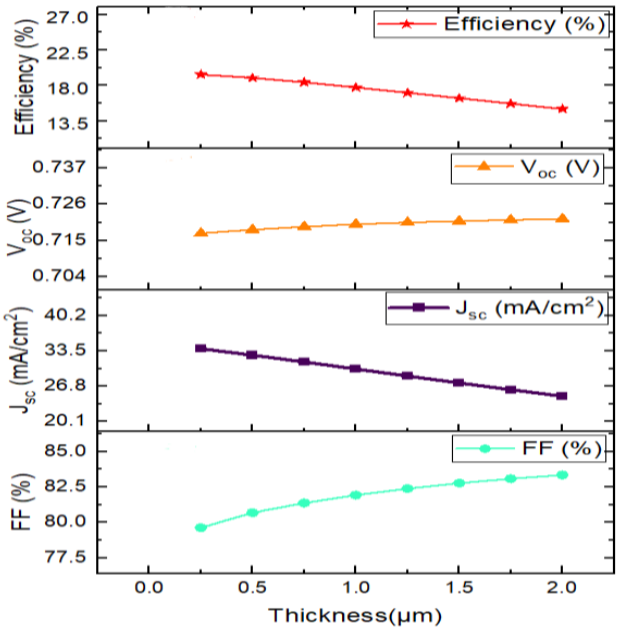

Fig. 2. Thickness variation of ZnSe

"Figure 2" below shows thickness variation of ZnSe window layer from 25 nm (1 μm = 1000 nm) to 200 nm and we observed the value of V_{oc} & FF was increased. On the other hand, the value of J_{sc} was decreased. So, the efficiency was decreased from 19.62% to 14.99 %. We Observed optimize value of thickness is 25 nm.

The ZnSe window layer generally has an ideal doping concentration range that balances the effectiveness of carrier extraction and collection. Doping concentration refers to the amount of dopant atoms added to a semiconductor material to modify its electrical properties.

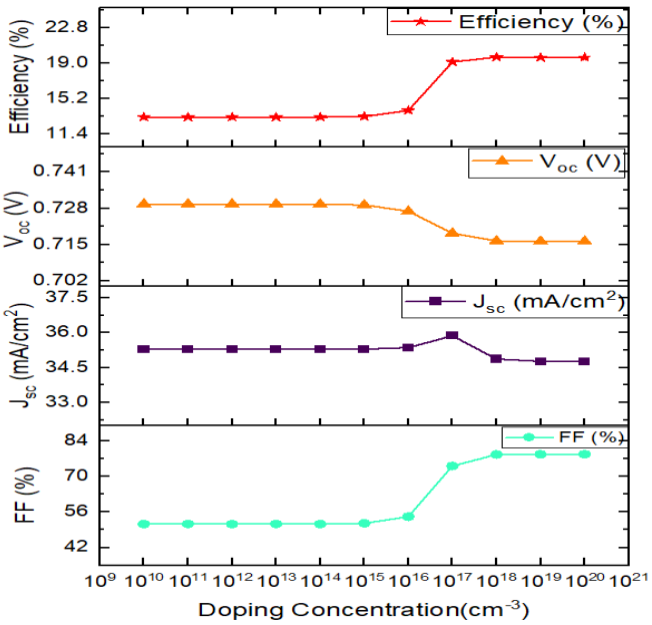

Fig. 3. Doping Concentration variation of ZnSe .

"Figure 3" displays the variance of doping concentration of ZnSe window layer from 10^{10} cm^{-3} to 10^{20} cm^{-3} and we observed almost the constant value of V_{oc} , J_{sc} & FF upto 10^{16} cm^{-3} doping concentration. As a result, the efficiency was almost same value from 10^{10} cm^{-3} to 10^{16} cm^{-3} then increased to highest 19.61 % for the of doping concentration 10^{10} cm^{-3}. Doping can increase the window layer's conductivity, facilitating efficient electron and hole transport. Higher conversion efficiency is the result of this easier separation of the photon generated carriers from the absorber layer. The exact solar cell design, materials employed and device structure affect doping concentration [38].

3.2. Impact of BSF Layer on Cell Performance

At solar cell's back surface, the BSF layer serves as a barrier to stop carrier recombination. By properly separating the photon generated electrons and holes in an area of high electric field, it decreases the likelihood of them recombining and lengthens their lifespan. The BSF layer aids in maximising the solar cell's total conversion efficiency by reducing carrier recombination [39]. Through the creation of a stronger electric field close to the back surface, the BSF layer improves carrier collecting. This field directs the photon generated carriers towards the direction of contacts, enabling effective extraction. A greater photocurrent results the better carrier collection, which boosts the solar cell's overall performance.

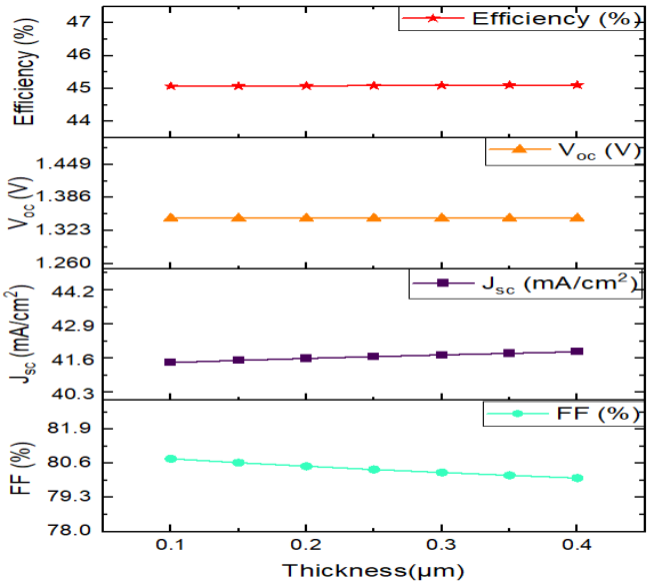

Fig. 4. Thickness variation of CGS

"Figure 4" shows the variation of thickness of CGS BSF layer from 100 to 400 nm, we observed almost constant value of V_{oc} & J_{sc} slightly increased. On the other hand the value of FF was decreased gradually. As a result, the efficiency remain almost constant at 45.08 %. 200 nm was selected for the cell's stable structure and cost-effectiveness.

Doping can also influence the bandgap of the CGS BSF layer. It is feasible to adjust the bandgap and electrical structure of CGS by varying doping concentration. As a result, this bandgap engineering can optimize the alignment with the absorber layer's bandgap, allowing for effective light absorption and carrier collection, and potentially boosting the solar cell's conversion efficiency. "Figure 5" shows variation of doping concentration of CGS from 10^{10} cm^{-3} to 10^{20} cm^{-3},

we observed almost the constant value of V_{oc}, J_{sc} & FF at 10^{17} cm^{-3}, as a result, the efficiency was almost constant. Afer increasing the value of doping concentration, efficiency slightly increased.

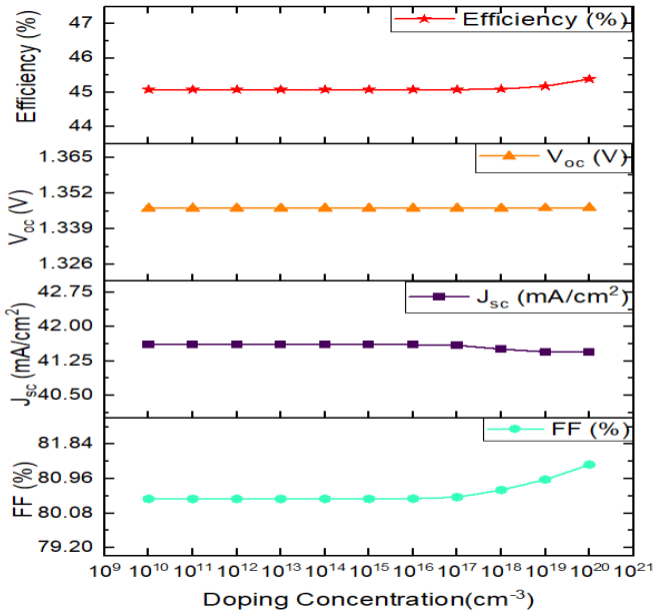

Fig. 5. Doping Concentration Variation of CGS

4. Variation of Defect Density for CZTS Solar Cell

As part of our inquiry into the impact of fault density, we have conducted experiments in which the value of imperfection density was changed from 10^{10} cm^{-3} to 10^{17} cm^{-3}, while ideal layer thickness remained same throughout the whole structure. Defect density is a measure of the number of structural imperfections within a material.

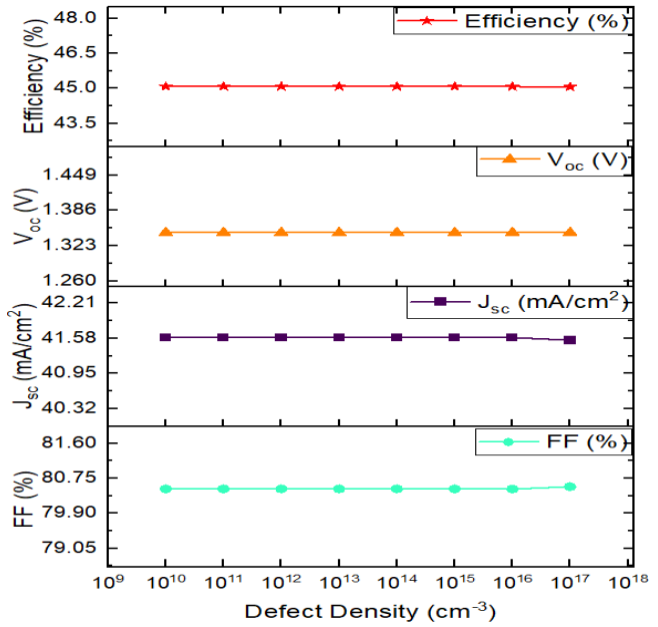

Fig. 6. Variation of Defect Density for CZTS Solar Cell

"Figure 6" shows the parameter curves for a number of different deficiency densities that were measured. This deterioration in quality may be linked to an increase in the recombination rate that happens with an increase in the defect density. Together, these two factors contribute to an overall rise in the defect density. In contrast, when the fault density is lower than 10^{17} cm^{-3} we saw almost constant values V_{oc}, J_{sc} & FF, as a result, the efficiency was almost constant at 45.08 %.

5. Temperature Variation's Impact on CZTS Solar Cell

Temperature evaporation has a significant influence on the output power of solar systems in thin-film solar cells [40, 41]. The variability of cell parameters is impacted by changes in operating temperature. The researchers looked at the thermal stability of the suggested solar cell in order to assess the potential of the CZTS absorber layer. "Figure 7" below shows the impact of operating temperature on efficiency from 250 K to 500K. The dual heterojunction cell's (n-ZnSe/p-CZTS/p^{+}-CGS/Ni) temperature coefficient is (-0.069 %/◦C) which denotes a good level of temperature stability.

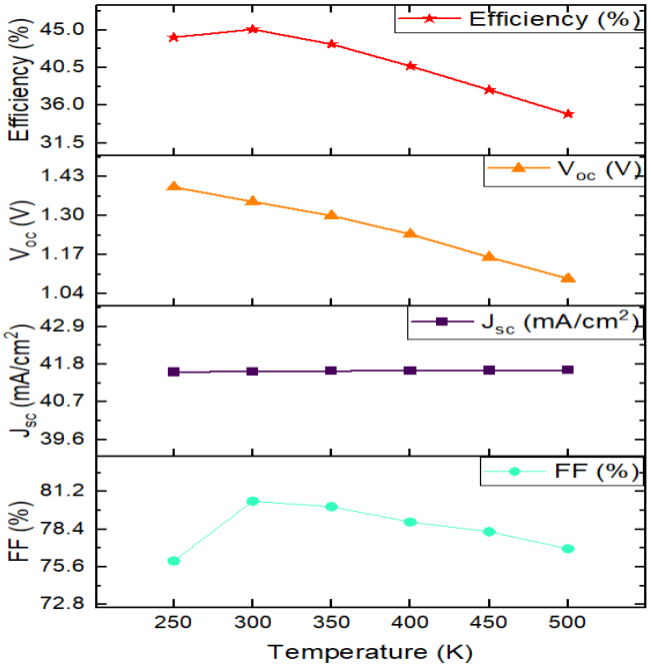

Fig. 7. Effects of operating temperature with BSF

6. JV Curve Characteristics

JV (current density-voltage) curve visually depicts the performance of a solar cell. Plotting the current density (J) vs the voltage (V) provides crucial information on the cell's open-circuit voltage, fill factor, short-circuit current density and efficiency. J-V curve characteristics for the suggested cell shape are displayed in "Figure 8". The graph indicates that the suggested cell structure performs better with BSF than without BSF.

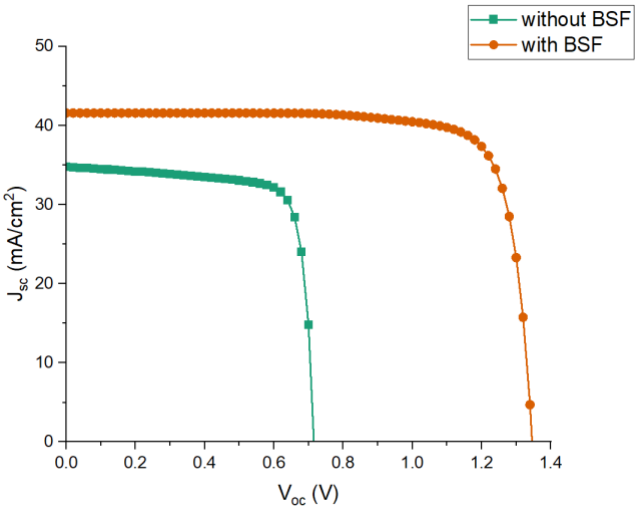

Fig. 8. Comparative study of J-V characteristics curve with and without BSF

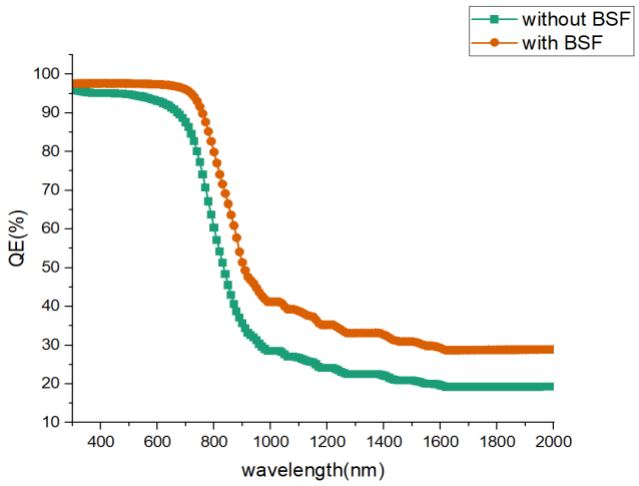

Fig.9. Quantum Efficiency of CZTS solar cell

7. Quantum Efficiency of CZTS Solar Cell

The capacity of a solar cell to convert photons of different wavelengths into electrical current is measured by its quantum effectiveness, or QE. The QE spectrum of a CZTS solar cell shows the percentage of photons that are absorbed and changed into charge carriers (electrons or holes) as a function of wavelength. Effective photon absorption and conversion to electrical current are indicated by a high QE, whereas inefficient absorption or significant losses are indicated by a low QE.

"Figure 9" illustrates that the quantum efficiency approaches 100% at wavelengths less than 600 nm due to the absorption coefficient of the most materials being higher at shorter wavelengths. This suggests that the material absorbs a higher percentage of photons with shorter wavelengths. As a result, more electron-hole pairs are created, raising the QE. The BSF layer, which also functions as the bottom absorber layer, absorbs photons with longer wavelengths using the TSA's two-step photo up conversion process. Furthermore, the BSF layer increases the intrinsic potential of the CZTS/CGS contact, which increases the V_{oc}. As such, quantum efficiency for dual heterojunctions is toward longer wavelengths in comparison to single heterojunctions without a BSF layer.

Table 2. Comparative table presenting recent research with various device configurations

Cell Structure	V_{oc} (V)	J_{sc} (mA/cm^2)	FF (%)	PCE (%)	Reference
n-ZnS/p-CZTS/p$^+$-WSe_2	0.96	33.72	83.75	27.31	[30]
n-CdS/p-CZTS/p$^+$-Si	0.68	23.71	65.97	10.69	[32]
n-In_2S_3/p- CZTS	0.43	8.3	52	1.85	[42]
n-ZnS/p-CZTS/p$^+$-Mo	0.38	17.19	46	3.02	[43]
n-In_2S_3/p- CZTS/p$^+$-Mo	0.62	20	54.5	6.9	[44]
n-ZnS/p-CZTS	0.73	20.27	58.59	8.94	[45]
n-CdS/p-CZTS/p$^+$-Mo	0.75	22.10	84.89	14.17	[46]
n-In_2S_3/p-CZTS/p$^+$-Au	0.67	25.85	82.24	14.41	[47]
n-ZnSe/p-CZTS/p$^+$-Mo	0.82	26.53	74.14	16.24	[48]
Perovskite/CZTS	1.18	24.79	88.36	25.95	[49]
n-ZnSe/p-CZTS/Ni	0.716	34.77	78.77	19.62	[This work]
n-ZnSe/p-CZTS/p$^+$-CGS/Ni	1.346	41.59	80.49	45.08	[This work]

8. Conclusion

In the simulation, the ZnSe window layer and the CGS BSF layer were employed to compare and optimize performance for the simulation of CZTS solar cells. The total efficiency of the single cell structure of n-ZnSe/p-CZTS/Ni structure is 19.62% with V_{oc}= 0.716V, J_{sc}=34.77 mA/cm^2, and FF=78.77 %. Efficiency for dual heterojunction cell structure of n-ZnSe/p-CZTS/p$^+$-CGS/Ni is 45.08 % with V_{oc}=1.346V, J_{sc}=41.59 mA/cm^2 and FF=80.49 %. Thermal stability is also assessed at each level, leading to the computation of the temperature coefficient at the end which is (-0.069 %/◦C) which can provide a cleaner alternative to fossil fuels and reducing the overall carbon footprint and promoting environmental sustainability.

References

[1] J. Collier, S. Wu and D. Apul, "Life cycle environmental impacts from CZTS (copper zinc tin sulfide) and Zn_3P_2 (zinc phosphide) thin film PV (photovoltaic) cells," *Energy*, pp. 314-321, 2014.

[2] M. A. Green, Y. Hishikawa, E. D. Dunlop, D. H. Levi, J. Hohl-Ebinger and A. W. Ho-Baillie, "Solar cell efficiency tables (version 52)," *Prog Photovolt Res Appl*, vol. 26, p. 427–436, 2018.

[3] R. Kishore, S. Singh and B. Das, "PECVD grown silicon nitride AR coatings on polycrystalline silicon solar cells," *Solar Energy Materials and Solar Cells*, vol. 26, no. 1-2, pp. 27-35, 1992.

[4] G. Willeke, H. Nussbaumer, H. Bender and E. Bucher, "A simple and effective light trapping technique for polycrystalline silicon solar cells," *Solar Energy Materials and Solar Cells*, vol. 26(4), pp. 345-356, 1992.

[5] M. Edoff, "Thin film solar cells: research in an industrial perspective," *Ambio*, vol. 41(Suppl 2), pp. 112-118, 2012.

[6] H. Uda, S. Ikegami and H. Sonomura, "Te—metal contact on evaporated CdTe film for a CdS/CdTe solar cell.," *Solar energy materials and solar cells*, vol. 35, pp. 293-298, 1994.

[7] N. K. Das, S. F. U. Farhad, J. Chakaraborty, A. K. S. Gupta, M. Dey and M. Al-Mam, "Structural and optical properties of RF-sputtered CdTe thin films grown on CdS: O/CdS bilayers," *International Journal of Renewable Energy Research*, vol. 10(1), pp. 293-302, 2020.

[8] S. A. Razi, N. K. Das, S. F. U. Farhad and M. A. M. Bhuiyan, "Influence of the $CdCl_2$ solution concentration on the properties of CdTe thin films.," *International Journal of Renewable Energy Research (IJRER)*, vol. 10(2), pp. 1012-1020, 2020.

[9] M. Dey, M. A. Matin, N. K. Das and M. Dey, "Germanium telluride as a BSF material for high efficiency ultra-thin CdTe solar cell," in *9th International Forum on Strategic Technology (IFOST),IEEE*, Cox's Bazar, Bangladesh, 2014.

[10] S. Bhattacharjee, M. Hassan, N. K. Das and M. Dey, "Design and Optimization of Copper Antimony Sulfide Thin Film Solar Cell," *International Journal of Renewable Energy Research (IJRER)*, vol. 13(3), pp. 1398-1405, 2023 Sep 27.

[11] M. Dey, R. Chakma, N. Rahman, M. Dey, N. K. Das, A. K. S. Gupta, M. A. Matin and N. Amin, "Study of ultra-thin and stable alsb solar cell with potential copper telluride BSF," in *In2017 IEEE Region 10 Humanitarian Technology Conference (R10-HTC) (pp. 811-814). IEEE*, Dhaka, Bangladesh, 2017 Dec 21.

[12] M. Dey, J. Ferdous, S. B. Afsar, M. Dey and N. K. Das, "Design and Optimization of Efficient FeS_2 Solar Cell," in *2019 International Conference on Electrical, Computer and Communication Engineering (ECCE), IEEE*, Cox'sBazar, Bangladesh, 2019.

[13] E. M. K. I. Ahamed, N. K. Das, A. K. S. Gupta, M. N. I. Khan, M. A. Matin and N. Amin, "Structural and optical characterization of As-grown and annealed $Zn_xCd_{1-x}S$ thin-films by CBD for solar cell applications," *International Journal of Renewable Energy Research*, vol. 10(3), pp. 1464-1474, 2020 Sep 23.

[14] M. Dey, M. Dey, S. Alam, A. K. S. Gupta, N. K. Das, M. A. Matin and N. Amin, "Design of ultra-thin CZTS solar cells with indium selenide as buffer layer," in *2017 International Conference on Electrical, Computer and Communication Engineering (ECCE) (pp. 946-950), IEEE*, Cox's Bazar, Bangladesh, 2017.

[15] M. Dey, M. Dey, S. Alam, N. K. Das, M. A. Matin and N. Amin, "Study of molybdenum sulphide as a novel buffer layer for CZTS solar cells," in *3rd International Conference on Electrical Engineering and Information*

Communication Technology (ICEEICT) (pp. 1-4). IEEE, Dhaka, Bangladesh, 2016.

[16] M. Dey, M. Dey, T. Biswas, S. Alam, N. K. Das, M. A. Matin and N. Amin, "Modeling of Cu_2ZnSnS_4 solar cells with Bismuth Sulphide as a potential buffer layer," in *5th International Conference on Informatics, Electronics and Vision (ICIEV), pp. 1095-1098. IEEE*, Dhaka, Bangladesh, 2016.

[17] U. Saha and M. K. Alam, "Proposition of an environment friendly triple junction solar cell based on earth abundant CBTSSe/CZTS/ACZTSe materials," *physica status solidi (RRL)–Rapid Research Letters*, vol. 12(1), p. 1700335, 2018.

[18] M. Ravindiran and C. Praveenkumar, "Status review and the future prospects of CZTS based solar cell–A novel approach on the device structure and material modeling for CZTS based photovoltaic device," *Renewable and Sustainable Energy Reviews*, vol. 94, pp. 317-29, 2018 Oct 1.

[19] H. Katagiri, K. Saitoh, T. Washio, H. Shinohara, T. Kurumadani and S. Miyajima, "Development of thin film solar cell based on Cu_2ZnSnS_4 thin films. ,, pp.," *Solar Energy Materials and Solar Cells*, Vols. 65(1-4), pp. 141-148, 2001.

[20] Y.-P. Lin, Y.-F. Chi, T.-E. Hsieh, Y.-C. Chen and K.-P. Huang, "Preparation of Cu_2ZnSnS_4 (CZTS) sputtering target and its application to the fabrication of CZTS thin-film solar cells," *Journal of Alloys and Compounds*, vol. 654, pp. 498-508, 2016.

[21] J. Henry, K. Mohanraj and G. Sivakumar, "Electrical and optical properties of CZTS thin films prepared by SILAR method," *Journal of Asian Ceramic Societies* , vol. 4(1), p. 81–84, 2016.

[22] Crovetto, M. K. Huss-Hansen and O. Hansen, "How the relative permittivity of solar cell materials influences solar cell performance," *Solar Energy*, vol. 149, pp. 145-150, 2017 Jun 1.

[23] S. Chen, X. G. Gong, A. Walsh and S. Wei, "Crystal and electronic band structure of Cu_2ZnSnX_4 (X= S and Se) photovoltaic absorbers: First-principles insights.," *Applied Physics Letters*, vol. 94(4), 2009.

[24] M. Kumar, A. Dubey, N. Adhikari, S. Venkatesan and Q. Qiao, "Strategic review of secondary phases, defects and defect-complexes in kesterite CZTS–Se solar cells," *Energy & Environmental Science*, vol. 8(11), pp. 3134-3159, 2015.

[25] K. Rudisch, Y. Ren, C. Platzer-Björkman and J. Scragg, "Order-disorder transition in B-type Cu_2ZnSnS_4 and limitations of ordering through thermal treatments," *Applied physics letters*, vol. 108(23), 2016 Jun 6.

[26] J. Chantana, H. Arai, Y. Niizawa and T. Minemoto, "Ohmic-like contact formation at the rear interface between Cu (In, Ga) Se_2 and ZnO: Al in a lift-off Cu (In, Ga) Se_2 solar cell," *Thin Solid Films*, vol. 616, pp. 17-22, 2016.

[27] S. P. Bremner, M. Y. Levy and C. B. Honsberg, "Analysis of tandem solar cell efficiencies under AM1. 5G spectrum using a rapid flux calculation method," *Progress in photovoltaics: Research and Applications*, vol. 16(3), pp. 225-233, 2008.

[28] A. Kuddus, A. Bakar, M. Ismail and J. Hossain, "Design of a highly efficient CdTe-based dual-heterojunction solar cell with 44% predicted efficiency," *Solar Energy Volume*, vol. 221, pp. 488-501, 2021 June.

[29] A. Martí and A. Luque, "Three-terminal heterojunction bipolar transistor solar cell for high-efficiency photovoltaic conversion," *Nature communications*, vol. 6902, p. 6(1), 2015.

[30] A. T. Abir, A. Joy, B. K. Mondal and J. Hossain, "Numerical prediction on the photovoltaic performance of CZTS-based thin film solar cell," *Nano select*, vol. 4(1), pp. 112-22, 2023 Jan.

[31] M. A. Sayeed and H. K. Rouf, "Numerical simulation of thin film solar cell using SCAPS-1D: ZnSe as window layer," in *In 2019 22nd International Conference on Computer and Information Technology (ICCIT) (pp. 1-5). IEEE*, Dhaka, Bangladesh, 2019, December.

[32] A. Cherouana and R. Labbani, "Numerical simulation of CZTS solar cell with silicon back surface field," *Materials Today: Proceedings*, vol. 5(5), pp. 13795-13799, 2018.

[33] Y. H. Khattak, F. Baig, B. Marí, S. Beg, S. R. Gillani and T. Ahmed, "Effect of CdTe back surface field on the efficiency enhancement of a CGS based thin film solar cell," *Journal of Electronic Materials*, vol. 47(9), pp. 5183-5190, 2018.

[34] S. Ishizuka, "$CuGaSe_2$ thin film solar cells: challenges for developing highly efficient wide-gap chalcopyrite photovoltaics.," *physica status solidi (a)*, vol. 216(15), p. 1800873, 2019.

[35] J. Song, S. Li, C. Huang, T. Anderson and O. Crisalle, "Modeling and simulation of a CuGaSe/sub 2//Cu(In/sub 1-x/,Ga/sub x/)Se/sub 2/ tandem solar cell," in *3rd World Conference onPhotovoltaic Energy Conversion, 2003. Proceedings of, Osaka, Japan, 2003, pp. 555-558 Vol.1.*, Osaka, Japan, 2003.

[36] A. M. E. Raj, S. M. Delphine, C. Sanjeeviraja and a. M. Jayachandran, "Growth of ZnSe thin layers on different substrates and their structural consequences with bath temperature," *Physica B: Condensed Matter*, vol. 405(10), p. 2485–2491, 2010.

[37] E. R. Shaaban, "Optical constants and fitted transmittance spectra of varies thickness of polycrystalline ZnSe thin films in terms of spectroscopic ellipsometry," *Journal of alloys and compounds*, vol. 563, pp. 274–279,, 2013.

[38] L. Yang, J. Zhu and a. D. Xiao, "Microemulsion-mediated hydrothermal synthesis of ZnSe and Fe-doped ZnSe quantum dots with different luminescence characteristics," *RSC advances*, vol. 2(21), p. 8179–8188, 2012.

[39] B. K. Mondal, S. K. Mostaque, M. A. Rashid, A. Kuddus, H. Shirai and a. J. Hossain, "Effect of CdS and In_3Se_4 BSF layers on the photovoltaic performance of PEDOT: PSS/n-Si solar cells: Simulation based on experimental data," *Superlattices and Microstructures* , vol. 152, p. 106853, 2021.

[40] F. Javed, "Impact of Temperature & Illumination for Improvement in Photovoltaic System Efficiency," *International Journal of Smart Grid - ijSmartGrid*, vol. 6(1), pp. 19-29, 2022.

[41] M. Dey, N. K. Das, M. Dey, S. F. U. Farhad, M. A. Matin and N. Amin, "Impact of Source to Substrate Distance on the Properties of Thermally Evaporated CdS Film," *International Journal of Renewable Energy Research (IJRER)*, vol. 11(1), pp. 495-503, 2021.

[42] V. G. Rajeshmon, N. Poornima, C. S. Kartha and K. P. Vijayakumar, "Modification of the optoelectronic properties of sprayed In_2S_3 thin films by indium diffusion for application as buffer layer in CZTS based solar cell," *Journal of alloys and compounds*, vol. 553, pp. 239-244, 2013 Mar.

[43] P. Prabeesh, V. G. Sajeesh, I. P. Selvam, M. S. D. Bharati, G. M. Rao and S. N. Potty, "CZTS solar cell with non-toxic buffer layer: A study on the sulphurization temperature and absorber layer thickness," *Solar Energy*, vol. 207, pp. 419-427, 2020.

[44] F. Jiang, C. Ozaki, Gunawan, T. Harada, Z. Tang, T. Minemoto, Y. Nose and S. Ikeda, "Effect of indium doping on surface optoelectrical properties of Cu2ZnSnS4 photoabsorber and interfacial/photovoltaic performance of cadmium free In_2S_3/Cu_2ZnSnS_4 heterojunction thin film solar cell," *Chemistry of Materials*, vol. 28(10), pp. 3283-3291, 2016.

[45] M. D. Wanda, S. Ouédraogo and J. M. B. Ndjaka, "Theoretical analysis of minority carrier lifetime and Cd-free buffer layers on the CZTS based solar cell performances," *Optik*, vol. 183, pp. 284-293, 2019.

[46] R. Mannu, S. Padhy and U. P. Singh, "Variation of different layer parameters in a CZTS based solar cell for optimum performance: A simulative approach," *Materials Today: Proceedings*, vol. 39, pp. 1876-1883, 2021.

[47] M. A. Ashraf and I. Alam, "Numerical simulation of CIGS, CISSe and CZTS-based solar cells with In_2S_3 as buffer layer and Au as back contact using SCAPS 1D," *Engineering Research Express*, vol. 2(3), p. 035015, 2020.

[48] A. Srivastava, P. Dua, T. R. Lenka and S. K. Tripathy, "Numerical simulations on CZTS/CZTSe based solar cell with ZnSe as an alternative buffer layer using SCAPS-1D," *Materials Today: Proceedings*, vol. 43, pp. 3735-3739, 2021.

[49] M. A. Shafi, L. Khan, S. Ullah, M. Y. Shafi, A. Bouich, H. Ullah and B. Mari, "Novel compositional engineering for~ 26% efficient CZTS-perovskite tandem solar cell," *Optik*, vol. 253, p. 168568, 2022.